

1 From Formal Boosted Tree Explanations to 2 Interpretable Rule Sets

3 Jinqiang Yu ✉ 

4 Department of Data Science and AI, Monash University, Australia
5 Australian Research Council OPTIMA ITTC, Australia

6 Alexey Ignatiev ✉ 

7 Department of Data Science and AI, Monash University, Australia

8 Peter J. Stuckey ✉ 

9 Department of Data Science and AI, Monash University, Australia
10 Australian Research Council OPTIMA ITTC, Australia

11 — Abstract —

12 The rapid rise of Artificial Intelligence (AI) and Machine Learning (ML) has invoked the need for
13 *explainable AI* (XAI). One of the most prominent approaches to XAI is to train rule-based ML models,
14 e.g. decision trees, lists and sets, that are deemed interpretable due to their transparent nature.
15 Recent years have witnessed a large body of work in the area of constraints- and reasoning-based
16 approaches to the inference of interpretable models, in particular decision sets (DSes). Despite being
17 shown to outperform heuristic approaches in terms of accuracy, most of them suffer from scalability
18 issues and often fail to handle large training data, in which case no solution is offered. Motivated by
19 this limitation and the success of gradient boosted trees, we propose a novel anytime approach to
20 producing DSes that are both accurate and interpretable. The approach makes use of the concept
21 of a generalized formal explanation and builds on the recent advances in formal explainability of
22 gradient boosted trees. Experimental results obtained on a wide range of datasets, demonstrate that
23 our approach produces DSes that more accurate than those of the state-of-the-art algorithms and
24 comparable with them in terms of explanation size.

25 **2012 ACM Subject Classification** Computing methodologies → Machine learning

26 **Keywords and phrases** Decision set; interpretable model; gradient boosted tree; BT compilation

27 **Digital Object Identifier** 10.4230/LIPIcs.CVIT.2016.23

28 **Supplementary Material** *Software (Source Code)*: <https://github.com/jinqiang-yu/cpl/>

29 **Acknowledgements** This research was partially funded by the Australian Government through the
30 Australian Research Council Industrial Transformation Training Centre in Optimisation Technologies,
31 Integrated Methodologies, and Applications (OPTIMA), Project ID IC200100009.

32 **1 Introduction**

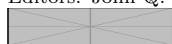
33 Rapid development of Artificial Intelligence (AI) and Machine Learning (ML) have revolu-
34 tionized all aspects of human lives in recent years [30, 1]. However, decisions made by most
35 widely used ML models are hard for humans to understand hence the interest in the theory
36 and practice of *Explainable AI* (XAI) rises.

37 One major approach to XAI is to compute *post-hoc* explanations for ML predictions
38 to answer a “*why*” question [34, 44], i.e. why the prediction is made. Although heuristic
39 approaches to post-hoc explanations prevail [34, 44, 43], they suffer from a number of
40 weaknesses [21, 16, 49, 52]. Formal methods [48, 20, 37] provide alternative approaches
41 to explanations that avoid these weaknesses. Another alternative approach to XAI is to
42 compute *interpretable* ML models, i.e. logic-based models, including decision trees [40],
43 decision lists [46], and decision sets [29]. These models enable decision makers to obtain



© ;
licensed under Creative Commons License CC-BY 4.0
42nd Conference on Very Important Topics (CVIT 2016).

Editors: John Q. Open and Joan R. Access; Article No. 23; pp. 23:1–23:22



Leibniz International Proceedings in Informatics
Schloss Dagstuhl – Leibniz-Zentrum für Informatik, Dagstuhl Publishing, Germany

44 succinct explanations from the models directly. In this paper, we focus on the decision
45 set (DS) models.

46 Decisions sets are particularly easy to explain: the rule that fired is an explanation of
47 the decision. This led to an upsurge in interest of decision sets that are both interpretable
48 and accurate. Recent work [50] uses propositional satisfiability (SAT) to generate minimum-
49 size decision sets that are perfectly accurate on the training data, and demonstrates that
50 decision sets that completely agree with the training data outperform others in terms of
51 accuracy. A more scalable maximum satisfiability (MaxSAT) approach [18] to this problem
52 was then proposed. Unfortunately, both of these methods are unable to provide any decision
53 information if a dataset is not completely solved.

54 Motivated by these works and their limitations, this paper aims at making a bridge
55 between formal post-hoc explainability and interpretable DS models. In particular, the paper
56 focuses on developing a novel anytime approach to computing decision sets that are both
57 interpretable and accurate, by compiling a gradient boosted tree model into a decision set
58 on demand with the use of formal explanations. This is done with the use of the recent
59 approach [17] to compute abductive explanations for gradient boosted trees using maximum
60 satisfiability (MaxSAT). Furthermore, the paper proposes a range of post-hoc model reduction
61 heuristics aiming at enhancing interpretability of the result models, done with MaxSAT
62 and integer linear programming (ILP). The experimental results show that compared with
63 other state-of-the-art methods, decision sets generated by the proposed approach are more
64 accurate, and comparable with the competition in terms of interpretability.

65 2 Preliminaries

66 **SAT and MaxSAT.** The standard definitions for propositional satisfiability (SAT) and
67 maximum satisfiability (MaxSAT) solving are assumed [3]. A propositional formula ϕ is
68 said to be in *conjunctive normal form* (CNF) if it is a conjunction of clauses. A *clause* is
69 a disjunction of literals, where a *literal* is either a Boolean variable b or its negation $\neg b$.
70 A *truth* assignment μ is a mapping from the set of variables to $\{0, 1\}$. A clause is said to
71 be *satisfied* by truth assignment μ if one of the literals in the clause is assigned value 1;
72 otherwise, the clause is *falsified*. If all clauses in formula ϕ are satisfied by assignment μ , ϕ is
73 satisfied; otherwise, assignment μ falsifies ϕ . A CNF formula ϕ is *unsatisfiable* if there exists
74 no assignment satisfying ϕ .

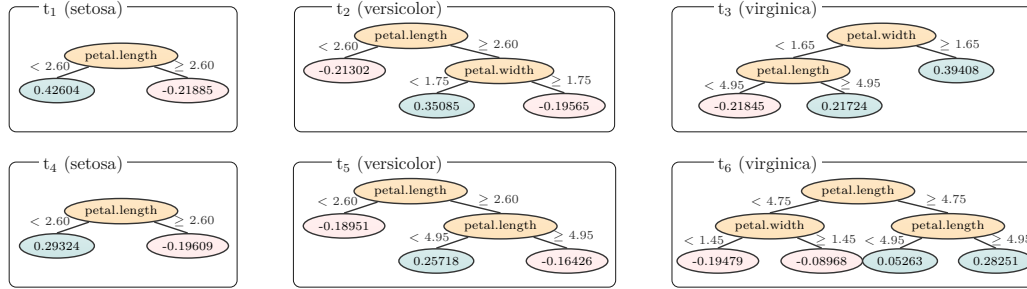
75 In the context of unsatisfiable formulas, the MaxSAT problem consists in finding a truth
76 assignment that maximizes the number of satisfied clauses. Hereinafter, we use a variant
77 of MaxSAT called Partial Weighted MaxSAT [3, Chapters 23 and 24]. The formula ϕ in
78 this variant is represented as a conjunction of *hard* clauses \mathcal{H} , which must be satisfied, and
79 *soft* clauses \mathcal{S} where each of them is associated with a weight representing a preference to
80 satisfy them, i.e. $\phi = \mathcal{H} \wedge \mathcal{S}$. Partial Weighted MaxSAT problems aim at finding a truth
81 assignment μ that satisfies all hard clauses and maximizes the total weight of satisfied soft
82 clauses.

83 **Classification Problems.** We consider classification problems with a set of classes¹ $\mathcal{K} =$
84 $\{1, \dots, k\}$, and a set of features $\mathcal{F} = \{1, \dots, m\}$. The value of each feature $i \in \mathcal{F}$ is taken
85 from its corresponding (numeric) domain D_i . As a result, the entire feature space is defined as
86 $\mathbb{F} \triangleq \prod_{i=1}^m D_i$. A concrete point represented by $\mathbf{v} = (v_1, \dots, v_m) \in \mathbb{F}$, s.t. each v_i is a constant

¹ Non-integer class labels can be mapped to a set $\{1, \dots, |\mathcal{K}|\}$.

IF “petal.length” < 2.60	THEN class = “setosa”
IF 2.60 ≤ “petal.length” < 4.95 ∧ “petal.width” < 1.75	THEN class = “versicolor”
IF “petal.length” ≥ 2.60 ∧ “petal.width” ≥ 1.75	THEN class = “virginica”
IF “petal.length” ≥ 4.95	THEN class = “virginica”

(a) Decision set



(b) BT model [5] consisting of 2 trees per class, each of depth ≤ 2, adopted from [17]

■ **Figure 1** Example DS and BT models computed on the well-known *Iris* classification dataset.

87 value taken by feature $i \in \mathcal{F}$, together with its corresponding class $c \in \mathcal{K}$, represented by a
 88 pair (\mathbf{v}, c) , indicate a *data instance* or *example*. With a slight abuse of notation and whenever
 89 convenient, a data point $\mathbf{v} \in \mathbb{F}$ is also referred to as an instance. Finally, $\mathbf{x} = (x_1, \dots, x_m)$
 90 denotes a vector of feature variables $x_i \in D_i$, $i \in \mathcal{F}$, used for reasoning over points in \mathbb{F} .

91 A classifier defines a *classification function* $\tau: \mathbb{F} \rightarrow \mathcal{K}$. The objective of classification
 92 problems is to learn a function τ to generalize well on unseen data given a training dataset $\mathcal{E} =$
 93 $\{e_1, e_2, \dots, e_n\}$, where each instance $e_d \in \mathcal{E}$ is a pair of (\mathbf{v}_d, c_d) . Classification problems are
 94 conventionally posed as an optimization problem, i.e. either to minimize the complexity of τ ,
 95 or maximize its accuracy, or both.

96 **Rules, Decision Sets and Gradient Boosted Trees.** Multiple ways exist to learn classifiers
 97 given data \mathcal{E} . This paper focuses on arguably one of the most interpretable models, i.e.
 98 decision sets, trained by *compiling* gradient boosted trees.

99 A *decision rule* is in the form of “IF antecedent THEN prediction”, where the antecedent
 100 is a set of feature literals. Informally, a rule is said to classify an instance $\mathbf{v} \in \mathbb{F}$ as class
 101 $c \in \mathcal{K}$ if its antecedent is *compatible* with \mathbf{v} (or *matches* \mathbf{v}) and its prediction is c . A *decision*
 102 *set* (DS) is an unordered set of decision rules \mathcal{R} . An instance $(\mathbf{v}, c) \in \mathcal{E}$ is misclassified by a
 103 DS if either there exists no rule in \mathcal{R} matching \mathbf{v} , or there exists a rule classifying \mathbf{v} as a
 104 class $c' \in \mathcal{K}$ s.t. $c' \neq c$.

105 A *gradient boosted tree* (BT) is a tree ensemble \mathfrak{T} defining sets of decision trees $T_c \in \mathfrak{T}$
 106 for each class $c \in [|\mathcal{K}|]$, where T_c comprises $N \in \mathbb{N}_{>0}$ trees t_{kz+c} , $z \in \{0, \dots, N-1\}$, $k \in [|\mathcal{K}|]$.
 107 Given an instance $\mathbf{v} \in \mathbb{F}$, its class is obtained by computing the sum of scores assigned by
 108 trees for each class $w(\mathbf{v}, c) = \sum_{t \in T_c} t(\mathbf{v})$ and assigning the class which has the maximum
 109 score, i.e. $\operatorname{argmax}_{c \in [|\mathcal{K}|]} w(\mathbf{v}, c)$. Whenever convenient, $\mathbf{n} \in t$ denotes a non-terminal node,
 110 where $t \in \mathfrak{T}$ represents an arbitrary decision tree. Moreover, each such \mathbf{n} indicates a feature
 111 condition in the form of $x_i < d$, where feature $i \in \mathcal{F}$ and *splitting threshold* $d \in D_i$.

► **Example 1.** Figure 1 shows DS and BT models trained on the *Iris* dataset, which has 4 numeric features and 3 classes: “setosa”, “versicolor”, and “virginica”. Observe that

■ **Table 1** Several instances extracted from *Iris* dataset.

#	sepal.length	sepal.width	petal.length	petal.width	class
e_1	5.1	3.5	1.4	0.2	setosa
e_2	7.7	2.6	6.9	2.3	virginica
e_3	5.6	2.5	3.9	1.1	versicolor
e_4	6.2	2.8	4.8	1.8	virginica
e_5	5.6	2.8	4.9	2.0	virginica

instance $\mathbf{v}_1 \in e_1$ shown in Table 1 is classified as “*setosa*” by the first rule of the DS. In the BT model, each class $c \in [3]$ is represented by 2 trees t_{3z+c} , $z \in \{0, 1\}$. Thus, it also classifies \mathbf{v}_1 as “*setosa*”, since the score of this class $w(\mathbf{v}_1, 1) = t_1 + t_4 = 0.71928$ is higher than the score of “*versicolor*” $w(\mathbf{v}_1, 2) = t_2 + t_5 = -0.40253$ and the score of “*virginica*” $w(\mathbf{v}_1, 3) = t_3 + t_6 = -0.41324$. \square

112 **Interpretability and Explanations.** Interpretability is not formally defined as it is considered
 113 to be a subjective concept [33]. In this paper interpretability is defined as the overall
 114 succinctness of the information offered by an ML model to justify a provided prediction.
 115 Moreover, following earlier work [48, 20], we equate explanations for ML models with *abductive*
 116 *explanations* (AXps), which are subset-minimal sets of features sufficient to explain a given
 117 prediction. Concretely, given an instance $\mathbf{v} \in \mathbb{F}$ and a prediction $c = \tau(\mathbf{v}) \in \mathcal{K}$, an AXp is a
 118 subset-minimal set of features $\mathcal{X} \subseteq \mathcal{F}$ such that

$$119 \quad \forall (\mathbf{x} \in \mathbb{F}). \left[\bigwedge_{i \in \mathcal{X}} (x_i = v_i) \right] \rightarrow (\tau(\mathbf{x}) = c) \quad (1)$$

► **Example 2.** Consider the setup of Example 1. Given instance \mathbf{v}_1 , observe that for any instance with “*petal.length*” = 1.4, the BT is guaranteed to predict “*setosa*” independently of the values of other features, since the weights for “*setosa*” and “*versicolor*” are 0.71928 and -0.40253 respectively as before, and the maximal weight for “*virginica*” is $0.39408 - 0.08968 = 0.30440$. Thus, the (only) AXp \mathcal{X} for the prediction for e_1 made by the BT model is $\{\text{“petal.length”}\}$. \square

120 **Explanations in BTs.** Formal reasoning has been recently applied to computing AXps for
 121 BT models, with the key difficulty being how to effectively reason about the aggregation
 122 over a large number of trees in a BT model. Recent work applied satisfiability modulo
 123 theory (SMT) [21] or mixed integer linear programming (MILP) solvers [42, 27] to directly
 124 address the linear summations arising in the BT encoding. Hereinafter, we build on the
 125 recent MaxSAT approach [17], which maps the aggregation reasoning to a set of MaxSAT
 126 queries to avoid a costly encoding of the linear constraints into CNF. Also, [17] demonstrates
 127 how a MaxSAT query can be made such that (1) holds if and only if the *optimal* value of
 128 the constructed objective function is negative.² In general, assuming that each feature $i \in \mathcal{F}$
 129 is numeric (continuous), the approach orders the set of splitting thresholds $\{d_{i1}, \dots, d_{ih_i}\}$
 130 in a BT \mathfrak{T} for each feature i , where h_i is the total number of thresholds of feature i in \mathfrak{T}
 131 and $d_{ij} \in \mathcal{D}_i$ for $j \in [h_i]$. Given an instance $\mathbf{v} = (v_1, \dots, v_m) \in \mathbb{F}$, the above approach
 132 associates each value v_i with a single interval I'_i from the set of disjoint intervals $\mathbb{D}_i = \{$
 133 $I_{i1} \equiv [\min(\mathcal{D}_i), d_{i1}), I_{i2} \equiv [d_{i1}, d_{i2}), \dots, I_{ih_i+1} \equiv [d_{ih_i}, \max(\mathcal{D}_i)] \}$. Thus, AXp extraction

² The reader is referred to [17] for the details.

134 boils down to finding a subset-minimal subset $\mathcal{X} \in \mathcal{F}$ s.t.

$$135 \quad \forall(\mathbf{x} \in \mathbb{F}). \left[\bigwedge_{i \in \mathcal{X}} x_i \in I'_i \right] \rightarrow (\tau(\mathbf{x}) = c) \quad (2)$$

► **Example 3.** Recall Example 2 and assume “*petal.length*” and “*petal.width*” have indices 3 and 4. Note that the sets of splitting thresholds for feature “*petal.length*” $\{d_{31} = 2.60, d_{32} = 4.75, d_{33} = 4.95\}$ and for feature “*petal.width*” $\{d_{41} = 1.45, d_{42} = 1.65, d_{43} = 1.75\}$. Let $\min(\mathcal{D}_3) = -\infty$ and $\min(\mathcal{D}_4) = 0.1$. Then we can associate the values of features 3 and 4 in our instance $\mathbf{v}_1 \in e_1$ with intervals $I_{31} \equiv (-\infty, 2.60)$ and $I_{41} \equiv [0.1, 1.45)$. Hence by (2), the AXp shown in Example 2 can in fact be seen as a rule $\langle IF \text{ “petal.length”} < 2.60 \text{ THEN class} = \text{“setosa”} \rangle$. □

136 **3** Related Work

137 Interpretable decision sets are logic-based ML models that can be traced back to the 70s and
 138 80s [39, 15, 4, 45]. To the best of our knowledge, [6] proposed the first approach to decision
 139 sets, which were introduced as the variant of decision lists [45, 7]. The first method making
 140 use of logic and optimization to synthesize a disjunction of rules that match a given dataset
 141 was proposed in [26]. Recent work [29] argued that decision sets are more interpretable than
 142 the other logic-based models, i.e. decision lists and decision trees. This work uses smooth
 143 local search to generate a set of rules first and heuristically minimizes a linear combination
 144 of criteria afterwards, e.g. the size of a rule, their maximum number, overlap or error.

145 Since then a number of works proposed the use of logic reasoning and optimization
 146 procedures to train DS models [22, 36, 12, 50, 18] claiming to significantly outperform the
 147 approach of [29] in terms of accuracy and performance. Among those, the works closest
 148 to ours are [22, 50, 18]. They proposed SAT-based approaches to computing smallest-size
 149 decision sets that *perfectly* agree with the training data by minimizing either the number
 150 of rules [22, 18] or the number of literals [50, 18] used in the model. Additionally, [50] is
 151 capable of computing *sparse* decisions sets that trade off training accuracy for model size.
 152 Despite the dramatic performance increase achieved in [18], all the approaches above suffer
 153 from scalability issues.

154 Post-hoc explainability is one of the major approaches to XAI. Besides a plethora of
 155 heuristic sampling-based methods to post-hoc explainability [43, 34, 44], a formal reasoning
 156 based approach to computing abductive explanations [48, 20] stands out. AXps can be
 157 related with prime implicants of the decision function (hence an alternative name *prime*
 158 *implicant explanations*, *PI-explanations*) associated with ML predictions and are guaranteed
 159 to capture the semantics of the ML models in the entire feature space. Although hard to
 160 compute in general, AXps were shown to be effectively computable for BT models by an
 161 incremental MaxSAT-based approach [17].

162 Our work aims at making a bridge between interpretable DS models and AXp computation
 163 by exploiting the latter for training the former. Given a BT model, it focuses on generating
 164 decision rules that agree with the BT. Each rule represents an AXp for the prediction made
 165 by the BT model, resulting in a DS model in a way *guided* by the original BT model. The
 166 approach is shown to outperform the prior logic-based approaches to DS inference in terms
 167 of test accuracy and performance. Note that despite prior attempts to train sparse models
 168 guided by tree ensembles [38], to our best knowledge, none of the existing works have applied
 169 formal post-hoc explanations to compile interpretable models.

170 Finally, our approach can be related to the existing line of work on *knowledge distilla-*
 171 *tion* [11, 13], where an interpretable model is trained to approximate a hard-to-interpret

black-box model, which is often seen as teacher-to-student knowledge transfer. Note that in contrast to knowledge distillation, our approach is able to *compile* a BT into an *equivalent* DS if we consider the entire feature space, as shown below.

4 Decision Sets by Boosted Tree Compilation

Based on [17], this section details a MaxSAT-based approach to compiling a BT into a DS where each rule in the DS is equivalent to a prime implicant of the BT classification function.

4.1 Rule Extraction

Recall that an AXp, as defined in (1) and (2), can be seen as an *if-then* rule. Given a hard-to-interpret BT model, the AXp extraction approach of [17] can be modified to compute an interpretable DS consisting of a *set* of AXps for the BT. However, when the features are continuous (numeric), this potential approach suffers from the following issue. Recall that an AXp $\mathcal{X} \in \mathcal{F}$ indicates a set of *concrete* feature values that are sufficient to explain a prediction $c = \tau(\mathbf{v})$ for a certain instance $\mathbf{v} \in \mathbb{F}$. Although this same AXp can explain other instances compatible with it, its applicability in general is at the mercy of expressivity of the feature literals used in the AXp, i.e. equality literals and succinct interval membership in the case of (1) and (2), respectively. Motivated by this limitation, we propose to compute AXps over the literals intrinsic to the BT model aiming at getting feature intervals that are as general as possible, as detailed below.³

In contrast to the work of [17], which associates each feature value $v_i \in D_i$ with a single *narrowest* interval I'_i covering the value, we exploit all the splitting points used by the BT for feature i and identify all of the corresponding literals satisfied by the feature value v_i . Note that the original MaxSAT encoding [17] introduces a single Boolean variable o_{ij} for each literal $x_i < d_{ij}$ with d_{ij} being a j 'th threshold used in the BT for feature i , s.t. $o_{ij} = 1$ iff $x_i < d_{ij}$ holds true. This way, each positive o_{ij} represents an upper bound on the value of x_i while each negative $\neg o_{ij}$ represents a lower bound on x_i .

► **Example 4.** Feature 3 (*“petal.length”*) from Example 3 has 3 thresholds: $d_{31} = 2.60$, $d_{32} = 4.75$, $d_{33} = 4.95$. Boolean variables o_{31} , o_{32} , and o_{33} are set to true iff $x_3 < 2.60$, $x_3 < 4.75$, and $x_3 < 4.95$, respectively. Let feature 3 take value 3.9 in the instance we want to explain. Observe how we can immediately assign literals $\neg o_{31}$, o_{32} , and o_{33} to true. ◻

Next, given an instance $\mathbf{v} = (v_1, \dots, v_m) \in \mathbb{F}$, let us construct a complete conjunction $\bigwedge_{i \in \mathcal{F}, j \in [h_i]} \tilde{o}_{ij}$ of literals \tilde{o}_{ij} s.t. \tilde{o}_{ij} is to be replaced by o_{ij} if $v_i < d_{ij}$ and replaced by $\neg o_{ij}$ otherwise. By construction, this conjunction holds true for instance \mathbf{v} . Now, given this conjunction of literals, we can apply the existing approach of [17] to extract a subset-minimal explanation $\mathcal{Y} \subseteq \{\tilde{o}_{ij} \mid i \in \mathcal{F}, j \in [h_i]\}$ for instance \mathbf{v} over literals \tilde{o}_{ij} s.t.

$$\forall (\mathbf{x} \in \mathbb{F}). \left[\bigwedge_{l \in \mathcal{Y}} l \right] \rightarrow (\tau(\mathbf{x}) = c) \quad (3)$$

Such an explanation \mathcal{Y} may (or may not) define either a lower bound on feature i , an upper bound, or both, aiming to construct the *most general* interval for each feature $i \in \mathcal{Y}$. Hence, we informally refer to such explanations as *generalized AXps* or simply *rules* (hereinafter, we use both interchangeably).

³ An alternative to our approach is *inflation* of abductive explanations, which is discussed in [23, 24]. Given an AXp, it aims at extending the set of values covered by each feature literal in the AXp while the AXp condition (1) still holds.

Algorithm 1 Deletion-based Rule Extraction

Function: RuleExtract($\mathfrak{T}, \mathbf{v}, c, \mathcal{E}$)**Input:** \mathfrak{T} : BT defining $\tau(\mathbf{x})$, \mathbf{v} : Instance, c : Prediction, i.e. $c = \tau(\mathbf{v})$ \mathcal{E} : Training data**Output:** \mathcal{Y} : Subset-minimal rule

```

1:  $\langle \mathcal{H}, \mathcal{S} \rangle \leftarrow \text{Encode}(\mathfrak{T})$ 
2:  $\mathcal{Y} \leftarrow \text{Init}(\mathfrak{T}, \mathbf{v})$ 
3:  $\mathcal{Y} \leftarrow \text{Sort}(\mathcal{Y}, \mathcal{E})$ 
4: for  $l \in \mathcal{Y}$  do
5:   if EntCheck( $\langle \mathcal{H}, \mathcal{S} \rangle, c, \mathcal{Y} \setminus \{l\}$ ) then
6:      $\mathcal{Y} \leftarrow \mathcal{Y} \setminus \{l\}$ 
7: return  $\mathcal{Y}$ 

```

► **Example 5.** Consider instance \mathbf{v}_3 predicted as “*versicolor*” by the BT (observe that $v_3 = 3.9$ and $v_4 = 1.1$) and recall the thresholds for features 3 and 4 discussed in Example 3. We can compute a generalized AXp $\mathcal{Y} = \{\neg o_{31}, o_{33}, o_{43}\}$ representing the second rule of the DS shown in Figure 1a. The original approach of [17] would instead compute an AXp defining the narrowest intervals for features 3 and 4, representing a rule: $\langle \text{IF } 2.60 \leq \text{“petal.length”} < 4.75 \wedge \text{“petal.width”} < 1.45 \text{ THEN class} = \text{“versicolor”} \rangle$, which is far less general than \mathcal{Y} . \square

207 A possible rule extraction procedure is outlined in Algorithm 1. (Please ignore line 3 for
 208 now; feature sorting is described in Section 4.2). The input BT model \mathfrak{T} is encoded into
 209 MaxSAT by applying the approach of [17]. Given an instance $\mathbf{v} \in \mathbb{F}$, the initial set of literals
 210 $\mathcal{Y} = \{\tilde{o}_{ij} \mid i \in \mathcal{F}, j \in [h_i]\}$ is created. Note that any feature $i \in \mathcal{F}$ unused in the BT \mathfrak{T} is
 211 excluded from \mathcal{Y} . The rest of the procedure implements the standard deletion-based AXp
 212 extraction [20], i.e. it iterates through all literals in \mathcal{Y} one by one, and checks which of the
 213 them can be safely removed such that entailment (3) still holds.

► **Example 6.** Consider our running example model and instance $\mathbf{v}_2 \in e_2$ from Table 1 predicted as “*virginica*” by the BT \mathfrak{T} . Given the thresholds for features 3 and 4 in Example 3, set \mathcal{Y} is initialized to $\{\neg o_{31}, \neg o_{32}, \neg o_{33}, \neg o_{41}, \neg o_{42}, \neg o_{43}\}$. The other two features are excluded from \mathcal{Y} since they are irrelevant to the classification function in \mathfrak{T} . Applying Algorithm 1 results in extracting a subset-minimal generalized AXp $\mathcal{Y} = \{\neg o_{33}\}$, which represents the rule $\langle \text{IF petal.length} \geq 4.95 \text{ THEN class} = \text{“virginica”} \rangle$. \square

214 ► **Remark 7.** Algorithm 1 relies on deciding whether formula (3) holds for each feature
 215 in explanation \mathcal{Y} . Here, this is done by means of a series of incremental core-guided
 216 MaxSAT oracle calls [19, 17]. One may wonder whether or not incomplete *anytime* MaxSAT
 217 solving [31, 35, 2, 32] can be applied in this setting. Although this may look plausible at
 218 first glance, time-restricted anytime MaxSAT algorithms can only *over-approximate* exact
 219 MaxSAT solutions while (3) holds *if and only if* the exact value of the objective function
 220 is negative. Therefore, an over-approximation of a MaxSAT solution is *never able* to prove
 221 the validity of (3) and so none of the features being tested can be discarded in the case of
 222 incomplete MaxSAT algorithms, which defies the purpose of Algorithm 1.

223 4.2 Boosted Tree Compilation

224 As mentioned above, generalized AXps can be seen as general decision rules that can be
 225 applied to an enormous number of instances. Therefore, it makes little sense to extract
 226 such rules for each instance in the feature space \mathbb{F} . Instead, one can devise an on-demand

Algorithm 2 Compile a BT into a DS

Function: $\text{Compile}(\mathfrak{T}, \tau, \mathcal{C})$ **Input:** \mathfrak{T} : BT defining $\tau(\mathbf{x})$, τ : Classification function in \mathfrak{T} , \mathcal{C} : Coverage set**Output:** \mathcal{R} : Set of Rules

```

1:  $\mathcal{R} \leftarrow \emptyset$ 
2:  $\mathcal{C}_u \leftarrow \mathcal{C}$ 
3: while  $\mathcal{C}_u \neq \emptyset$  do
4:    $\mathbf{v} \leftarrow \text{GetInst}(\mathcal{E}_u)$ 
5:    $\mathcal{Y} \leftarrow \text{RuleExtract}(\mathfrak{T}, \mathbf{v}, c = \tau(\mathbf{v}), \mathcal{E}_u)$ 
6:    $\mathcal{C}_c \leftarrow \text{GetCover}(\mathcal{Y}, \mathcal{C}_u)$ 
7:    $\mathcal{C}_u \leftarrow \mathcal{C}_u \setminus \mathcal{C}_c$ 
8:    $\mathcal{R} \leftarrow \mathcal{R} \cup \mathcal{X}'$ 
9: return  $\mathcal{R}$ 

```

227 *compilation* process, i.e. given a *yet uncovered* instance $\mathbf{v} \in \mathbb{F}$, we can apply Algorithm 1 to
 228 extract a rule covering \mathbf{v} (and some other instances). Clearly, *exhaustive* compilation of a
 229 BT, i.e. if the target is to cover all the instances in \mathbb{F} with generalized AXps of the BT, is
 230 computationally expensive given that AXp extraction for tree ensembles is hard for D^P [25].
 231 This can also lead to the large size of the resulting DSes making them hard to interpret. In
 232 practice, *local* compilation aiming at capturing the behavior of the BT on the training data
 233 only, is sufficient to generate a DS, which is both accurate and interpretable.

234 The proposed approach to compiling a BT \mathfrak{T} into a DS \mathcal{R} is shown in Algorithm 2.
 235 We initialize the set \mathcal{C}_u of currently uncovered instances to be equal to \mathcal{C} , i.e. the set of
 236 examples we wish to cover. The algorithm represents a loop generating rules until the set of
 237 computed rules \mathcal{R} covers all instances in coverage set data \mathcal{C}_u , i.e. until there is no uncovered
 238 instances in \mathcal{C} . Each iteration of the algorithm selects an instance \mathbf{v} from \mathcal{C}_u . Afterwards,
 239 a generalized AXp \mathcal{Y} for the prediction $c = \tau(\mathbf{v})$ by the BT \mathfrak{T} (recall that \mathfrak{T} is meant to
 240 compute classification function $\tau(\mathbf{x})$) is extracted by invoking Algorithm 1. The iteration
 241 proceeds by updating the set of rules \mathcal{R} and the set of uncovered instances \mathcal{C}_u . The algorithm
 242 terminates when all the instances in the coverage set \mathcal{C} are covered and returns a compiled
 243 DS \mathcal{R} .

244 ► **Proposition 8.** *Let \mathfrak{T} be a BT and \mathcal{R} be a DS returned by Algorithm 2 for \mathfrak{T} . Then $\mathcal{R} \equiv \mathfrak{T}$
 245 with respect to \mathcal{C} .*

246 We consider two usages of the algorithm: for *exhaustive compilation* the coverage set $\mathcal{C} = \mathbb{F}$
 247 is all possible feature combinations (in practice we model this coverage set implicitly, rather
 248 than in its explicit exponential sized form), and for *training set compilation* where $\mathcal{C} = \mathcal{E}$ is
 249 the training set. Based on the properties of prime implicants, Proposition 8 states that as a
 250 generalized AXp $\mathcal{Y} \in \mathcal{R}$ is a formal explanation for a prediction made by BT \mathfrak{T} , a compiled
 251 DS captures the semantics of the original model \mathfrak{T} on *coverage set* \mathcal{C} , assuming everything
 252 else is a *don't care*. Furthermore, if the process is applied subject to coverage set $\mathcal{C} = \mathbb{F}$,
 253 i.e. when we target the entire feature space \mathbb{F} , then \mathcal{R} and \mathfrak{T} behave identically, i.e. they
 254 compute the same classification function $\tau(\mathbf{x})$.

255 ► **Corollary 9.** *Let Algorithm 2 return a DS \mathcal{R} for a BT \mathfrak{T} . Then there is no instance
 256 in feature space \mathbb{F} covered by two distinct rules $\mathcal{Y}_1, \mathcal{Y}_2 \in \mathcal{R}$ predicting inconsistent classes
 257 $c_1 \neq c_2$.*

258 As each generalized AXp for \mathfrak{T} represents a prime implicant of the decision function $\tau(\mathbf{x})$

259 computed over literals \tilde{o}_{ij} , the above corollary claims that there are no overlapping rules in
 260 the result DS \mathcal{R} . This contrasts with other modern approaches to DS inference, where rule
 261 overlap is known to be a problem [29, 22]. Note that this approach still suffers from another
 262 common issue of DS models: namely, if DS \mathcal{R} is computed for the training data \mathcal{E} , there
 263 may still be instances in \mathbb{F} uncovered by \mathcal{R} .

► **Example 10.** Consider the running example BT model shown in Figure 1b. Its compiled
 DS representation computed by Algorithm 2 is shown in Figure 1a. Observe that there is
 no rule overlap in the DS computed. In fact, as the DS is computed by taking into account
 feature space \mathbb{F} , it computes the same classification function as the original BT model. ◻

264 **Feature Sorting.** Intuitively, how general and hence how applicable a rule is depends on
 265 how frequently the features used in it appear in the training data \mathcal{E} labeled with the target
 266 class. Thus, a simple heuristic to apply when extracting a rule for prediction $c = \tau(\mathbf{v})$ is to
 267 sort the initial state of $\mathcal{Y} = \{\tilde{o}_{ij} \mid i \in \mathcal{F}, j \in [h_i]\}$ based on how frequently the corresponding
 268 literals \tilde{o}_{ij} apply in examples \mathcal{E} labeled with c . This feature sorting represented by line 3 in
 269 Algorithm 1 in practice (according to our experiments) results in significantly more general
 270 rules and so overall smaller DSes.

271 **Anytime Property.** Most widely used reasoning-based algorithms to infer DSes provide
 272 a solution only if the computation is completed; otherwise, no decision set is reported. In
 273 contrast to these, the proposed approach is an *anytime* algorithm, i.e. it can return a *valid*
 274 DS \mathcal{R} even though the compilation process is interrupted before all the coverage set instances
 275 \mathcal{C} are covered. Furthermore, it can generate a more comprehensive DS \mathcal{R} , which covers more
 276 instances as it keeps going, i.e. after we have covered $\mathcal{C} \subseteq \mathbb{F}$ we can continue running the
 277 algorithm for the (unseen) instances of \mathbb{F} .

278 4.3 Post-Hoc Model Reduction

279 The compiled DS \mathcal{R} can be large (in terms of either the number of rules or the total number
 280 of literals) since each generalized AXp $\mathcal{Y} \in \mathcal{R}$ may need a significant number of literals to
 281 explain a prediction made by BT \mathfrak{T} , or/and many rules are required to explain all instances
 282 of \mathcal{C} . Once the target DS is obtained, we can apply post-hoc heuristic methods for reducing
 283 its size and so making it more interpretable. The methods below are in a way inspired by
 284 the optimization problems studied in [18, 50]. Although these ideas are applicable to any DS
 285 inference method once the result model is devised, they do not look necessary for standard
 286 DS inference algorithms as they minimize the model while training. On the contrary, no
 287 minimization is applied in the rule enumeration process described above and so post-hoc
 288 model reduction plays a vital role in our approach to reduce the size of final DS models.

289 **Reducing the Number of Rules.** Given a set of rules \mathcal{R} , we can compute a minimum
 290 subset $\mathcal{R}^* \subseteq \mathcal{R}$ that is still equivalent to the BT \mathfrak{T} wrt. the coverage set \mathcal{C} using discrete
 291 optimization, e.g. integer-linear programming (ILP). Concretely, the approach aims at
 292 selecting the smallest-size subset $\mathcal{R}^* \subseteq \mathcal{R}$ that covers all instances in \mathcal{C} , where \mathcal{R} is the
 293 compiled DS from \mathfrak{T} . Here, the size of \mathcal{R}^* is measured as the total number of literals used.
 294 This can be done by solving the following *set cover problem* [28]. Namely, for each rule
 295 $\mathcal{Y}_j \in \mathcal{R}$, we introduce a Boolean variable u_j such that $u_j = 1$ iff \mathcal{Y}_j is included in \mathcal{R}^* .
 296 Additionally, a Boolean variable y_{ij} is used to indicate that \mathcal{Y}_j covers $e_i \in \mathcal{C}$. As a result,

297 the weighted set cover problem for minimizing the total number of literals used is as follows:

$$298 \quad \text{minimize} \quad \sum_{j=1}^{|\mathcal{R}|} (|\mathcal{Y}_j| + 1) \cdot u_j \quad (4)$$

$$299 \quad \text{subject to} \quad \forall_{i \in [n]} \sum_{j=1}^{|\mathcal{R}|} y_{ij} \cdot u_j \geq 1 \quad (5)$$

300

301 **Reducing the Number of Literals.** Additionally, one can minimize the total number of
 302 literals used in the rules of \mathcal{R} . Given a rule $\mathcal{Y} \in \mathcal{R}$, this can be done either lexicographically
 303 by maximizing rule accuracy followed by size minimization, or by optimizing both, or trading
 304 off misclassifications for rule size – in either case, a single MaxSAT call per rule to minimize
 305 can be made. The intuition is that if a rule \mathcal{Y} misclassifies k instances then its optimized
 306 version $\mathcal{Y}^* \subseteq \mathcal{Y}$ should not result in many more misclassifications on training data \mathcal{E} . Recall
 307 that a rule misclassifies an instance $\mathbf{v}_k \in \mathcal{C}$ if it matches \mathbf{v}_k but assigns it to a wrong class.

308 Inspired by [18], we introduce a Boolean variable p_k , which is true iff rule \mathcal{Y} covers \mathbf{v}_k —
 309 this holds if \mathcal{Y} does not use any literals incompatible with \mathbf{v}_k . If $\mathcal{Y}_{\mathbf{v}_k} = \{\tilde{o}_{ij} \mid i \in \mathcal{F}, j \in [h_i]\}$
 310 are all the literals compatible with \mathbf{v}_k then this can be modeled with constraints

$$311 \quad \forall_{k \in [|\mathcal{C}|]} p_k \leftrightarrow \bigwedge_{l \in \mathcal{Y} \setminus \mathcal{Y}_{\mathbf{v}_k}} \neg l \quad (6)$$

312 Furthermore, let rule \mathcal{Y} predict $c \in \mathcal{K}$ and let $\mathcal{C}_\Theta \subseteq \mathcal{C}$ contain all instances labeled with any
 313 other class. Thus, we can apply the objective below when minimizing rule \mathcal{Y} :

$$314 \quad \sum_{l \in \mathcal{Y}} l + \sum_{k \in [|\mathcal{C}_\Theta|]} W \cdot p_k \quad (7)$$

315 If W is large enough, say $|\mathcal{C}| + 1$, this lexicographically minimizes misclassifications and then
 316 literals. If W is small, e.g. $1/\lambda \cdot |\mathcal{C}|$, this trades off $\lambda \cdot |\mathcal{C}|$ misclassifications for one literal.

317 **5 Experimental Results**

318 This section compares the proposed approach with the state-of-the-art DS learning algorithms
 319 on a variety of publicly available datasets in terms of accuracy, scalability, model and
 320 explanation size. The experiments are performed on an Intel Xeon 8260 CPU running
 321 Ubuntu 20.04.2 LTS, with the time limit of 3600s and the memory limit of 8GByte. Our
 322 experiments contain two parts, namely, exhaustive BT compilation and training-set BT
 323 compilation.

324 **Prototype implementation.** A prototype of the compilation-based approach to generating
 325 DSeS was developed as a set of Python scripts using $\mathcal{C} = \mathcal{E}$, hereinafter referred to as *ctl*.
 326 The implementation of BT compilation exploits [17] and, therefore, makes use of the RC2
 327 MaxSAT solver [19].⁴ The BTs to be compiled are computed by XGBoost [5]; the number
 328 of trees per class in a BT model is 50 and the maximum depth of each tree is 3. Post-hoc
 329 literal reduction is done again with RC2 [19]. Let *ctl* denote the implementation applying

⁴ Real weights in the objective function are not conventionally supported by MaxSAT solvers; the only other solver to support real weights besides RC2 is LMHS [47].

330 lexicographic optimization while $cpl_{l\lambda_1}$ trades off model accuracy for the number of literals
 331 used, with $\lambda_1 = 0.005$. Let cpl_r denote the implementation with post-hoc rule reduction
 332 applied using the Gurobi ILP solver [14]. The configuration with both post-hoc lexicographic
 333 optimization and rule reduction is denoted cpl_{lr} . Finally, the proposed approach applying
 334 exhaustive compilation $\mathcal{C} = \mathbb{F}$ is referred to as cpl_f .

335 **Competition.** Our approach is compared against: *twostg* a two-stage MaxSAT approach [18]
 336 for DSes perfectly accurate on the training data; *opt* another MaxSAT approach [50] for
 337 perfectly accurate DSes; sp_{λ_1} a sparse alternative to *opt* by the same authors (with $\lambda_1 = 0.005$)
 338 optimizing like $cpl_{l\lambda_1}$; *imli*₁ and *imli*₁₆ using MaxSAT-based IMLI [12] to minimize the
 339 number of literals given a predefined number of rules (we use 1 or 16); *ids* a state-of-the-
 340 art approach [29] based on smooth local search;⁵ *ripper* a popular heuristic DS algorithm
 341 RIPPER [8]; and CN2 (referred to as *cn2*) another heuristic algorithm [7, 6].⁶

342 **Datasets.** For the evaluation, 59 publicly available datasets from UCI Machine Learning
 343 Repository [9] and Penn Machine Learning Benchmarks [41] are considered. We apply 5-fold
 344 cross validation, resulting in 295 pairs of training and test (unseen) data. For the sake of a fair
 345 comparison, the datasets used are preprocessed so that each original feature $i \in \mathcal{F}$ is replaced
 346 with a number of non-intersecting feature intervals $x_i < d_{ij}$ defined by the XGBoost model
 347 (see Section 2). This guarantees that all competitors tackle the same problem instances.

348 5.1 Exhaustive BT Compilation

349 The first experiment compares exhaustive compilation, where $\mathcal{C} = \mathbb{F}$ is the entire feature
 350 space. This is impractical except for 6 small benchmarks.

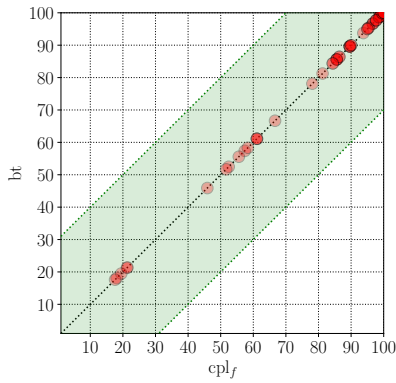
351 **Results.** Here we compare cpl_f with the competition in terms of accuracy, the total number
 352 of literals used and explanation size. We present the results as cactus plots showing the
 353 number of datasets that e.g. reach a certain accuracy, or finish in a certain runtime, for each
 354 method. These experimental results are shown in Figures 2 and 3 as well as the average
 355 results across folds are described in Table 2 where only the results of the datasets *completely*
 356 solved by compared competitors are presented. Note that cpl_f is nowhere near as scalable as
 357 the approaches described in the later experiments, but it is the *most accurate* approach to
 358 creating DSes we are aware of.

359 **Test accuracy.** An instance is considered misclassified if either there exists a rule of a
 360 wrong class that covers it, or it is not covered by any rule of the correct class. Thus, the test
 361 accuracy in this paper is calculated as $\frac{n-g}{n}$, where n is the total number of instances in the
 362 test data and g is the total number of misclassified instances. If an approach fails to train a
 363 model within the time limit, we assume its accuracy to be 0% for this dataset.

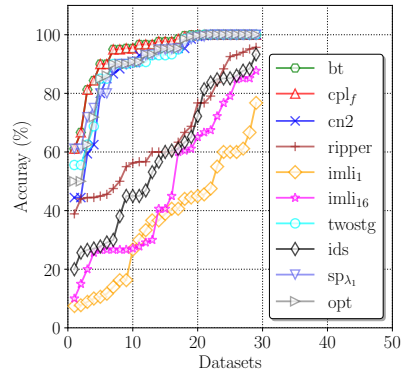
364 As can be seen in Figure 2b and Table 2, the best accuracy is achieved by BTs and cpl_f .
 365 In fact, these models share the same accuracy (this is also confirmed in Figure 2a), which

⁵ Since the original implementation performs poorly [22], here we consider the new implementation of IDS [10], which is claimed to be orders of magnitude faster than the original implementation.

⁶ Note that since RIPPER and IMLI compute a single class only given the training data, both of these competitors are augmented with a default rule predicting a class (1) different from the target class and (2) represented by the majority of training instances. Other algorithms, including our approach, incorporate a default rule that assigns a class based on the majority class in the training instances.

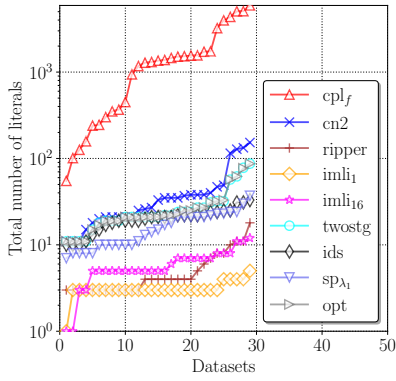


(a) Comparison with BT

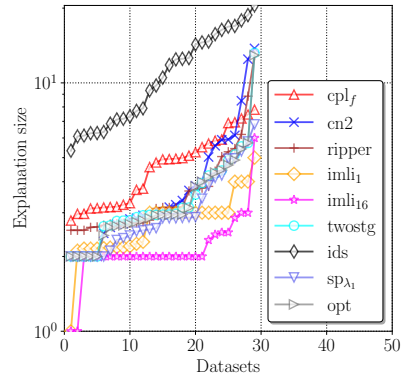


(b) Comparison with the others

■ **Figure 2** Accuracy of exhaustive compilation. The *standard* interpretation of cactus plots is assumed, i.e. a plot sorts the datapoints for each method by the y -axis value, and then shows them in increasing order independently of other methods. Thus, the order of datasets/folds differs for different methods. Also, the order of datasets for the same method differs in different subplots.



(a) Number of literals used



(b) Explanation size

■ **Figure 3** Succinctness of exhaustive compilation.

366 should not come as a surprise given that cpl_f replicates the behavior of the BT in the entire
 367 feature space \mathbb{F} (see Proposition 8).

368 **Model Complexity.** In general, complexity of a DS model can be measured by the total
 369 number of literals used in this DS. The total number of literals used in DS models is compared
 370 in Figure 3a and Table 2. Though the accuracy of DSEs trained by cpl_f outperforms the
 371 other competitors, these models are significantly larger, which is no surprise given that cpl_f
 372 computes many more rules with no post-hoc reduction applied.

373 **Explanation size.** Explanation size is defined as the number of literals required to explain
 374 an instance.⁷ This is arguably more important than the model size, since it defines “how
 375 hard” it is to understand an individual explanation. A small DS model tends to provide

⁷ See [51] for details.

■ **Table 2** Accuracy, number of literals used, and explanation size across folds.

Approach	Dataset					
	cardiotocography	hayes-roth	iris	new-thyroid	orbit	zoo
	Accuracy (%)					
bt	100.0	84.38	96.0	96.74	99.66	96.0
<i>cpl_f</i>	100.0	84.38	96.0	96.74	99.66	96.0
<i>sp_{λ₁}</i>	100.0	73.44	94.0	91.63	99.43	89.05
<i>opt</i>	100.0	70.63	93.33	91.63	99.54	93.05
<i>twostg</i>	100.0	71.25	92.67	92.09	99.54	91.1
<i>cn2</i>	100.0	62.5	92.67	93.02	99.54	89.1
<i>ripper</i>	45.3	66.25	57.33	80.93	94.11	60.33
<i>ids</i>	27.23	43.75	58.67	76.28	85.29	40.62
<i>imli₁₆</i>	27.23	38.75	25.34	69.77	70.55	43.33
<i>imli₁</i>	45.3	39.37	32.67	26.98	8.93	60.33
	Number of literals used					
<i>cpl_f</i>	3120.0	76.0	214.0	3614.2	729.8	1422
<i>sp_{λ₁}</i>	21.0	33.5	9.0	15.4	10.0	23.2
<i>opt</i>	21.0	63.6	19.4	23.0	11.8	30.0
<i>twostg</i>	21.0	64.2	19.8	22.6	11.8	29.8
<i>cn2</i>	21.0	116.2	27.2	36.6	13.2	40.8
<i>ripper</i>	3.0	12.8	5.0	8.2	4.0	3.0
<i>ids</i>	21.0	21.6	19.8	20.0	25.0	14.2
<i>imli₁₆</i>	5.0	2.2	7.4	7.4	6.4	5.0
<i>imli₁</i>	3.0	2.2	3.0	4.2	3.0	3.0
	Explanation size					
<i>cpl_f</i>	7.26	3.76	3.02	4.9	3.18	5.4
<i>sp_{λ₁}</i>	2.0	6.31	2.45	4.13	2.86	3.64
<i>opt</i>	2.0	5.41	2.76	4.3	2.94	2.96
<i>twostg</i>	2.0	5.4	2.87	4.23	2.94	3.33
<i>cn2</i>	2.0	6.94	3.02	4.47	3.02	4.05
<i>ripper</i>	2.73	10.15	4.3	4.3	3.15	2.59
<i>ids</i>	16.08	18.23	13.06	7.74	6.23	9.28
<i>imli₁₆</i>	2.0	2.2	2.1	1.97	2.8	2.46
<i>imli₁</i>	2.18	2.2	3.0	4.0	3.0	2.2

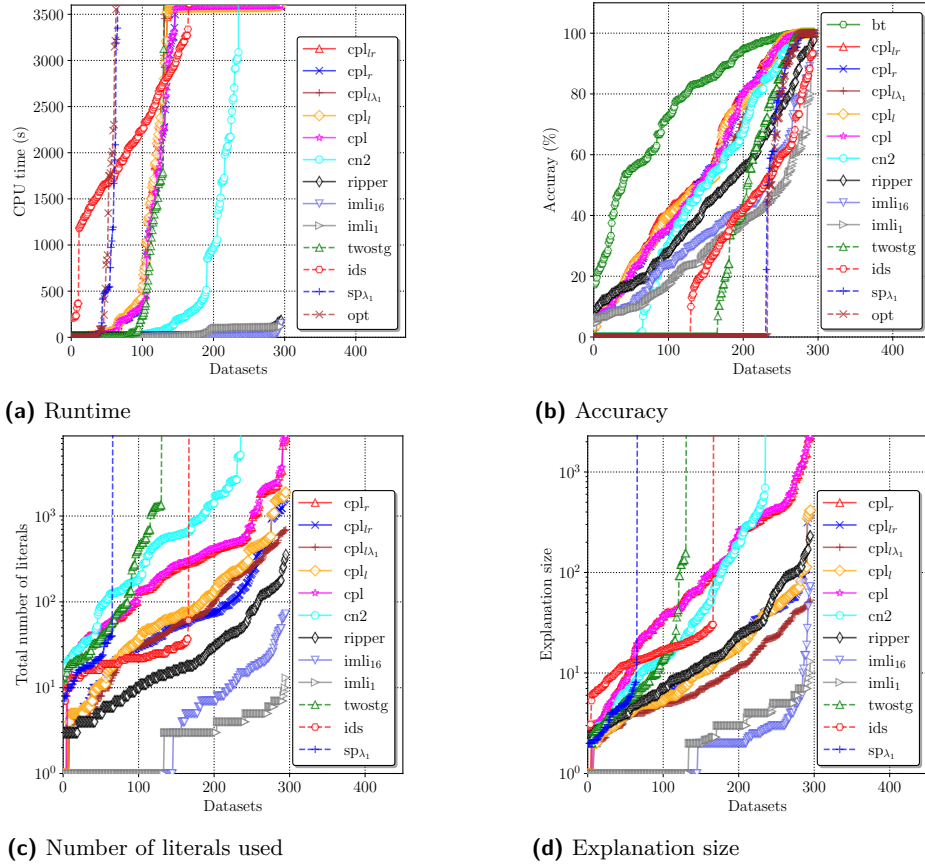
376 compact explanations but it is not always accurate. As can be seen in Figure 3b and Table 2
 377 and similar to the total number of literals used in DSes, *cpl_f* requires more literals to explain
 378 an instance than all competitors except *ids*.

379 A crucial observation to make here is that we test explanation size for each of the test
 380 instances available. Although test data are meant to extrapolate the overall unseen data,
 381 such approximation of the unseen feature space is not ideal. As a result, there may be
 382 numerous instances in \mathbb{F} *uncovered* by all the approaches but *cpl_f*, in which case it will
 383 be the *only* approach providing a user not only with a prediction but also with a succinct
 384 explanation of the prediction made.

385 5.2 BT Compilation Targeting Training Data

386 Compilation to cover the training set $\mathcal{C} = \mathcal{E}$ is much more efficient, and the main usage we
 387 expect of our algorithms.

388 **Scalability.** Figure 4a depicts scalability of all selected algorithms on the 295 considered
 389 datasets. Note that runtime of our approach includes BT training time. The best performance
 390 is demonstrated by the proposed implementation, i.e. *cpl* and *cpl_{*}*, $* \in \{l, r, lr, l\lambda_1\}$, where
 391 all selected datasets are solved within the time limit. This is not surprising since the approach
 392 is an anytime algorithm that can always return a valid DS. As for other competitors, the
 393 heuristic method *ripper* and the MaxSAT approaches *imli₁* as well as *imli₁₆* also solve all
 394 considered datasets. Next is the heuristic algorithm *cn2*, where 235 datasets are solved

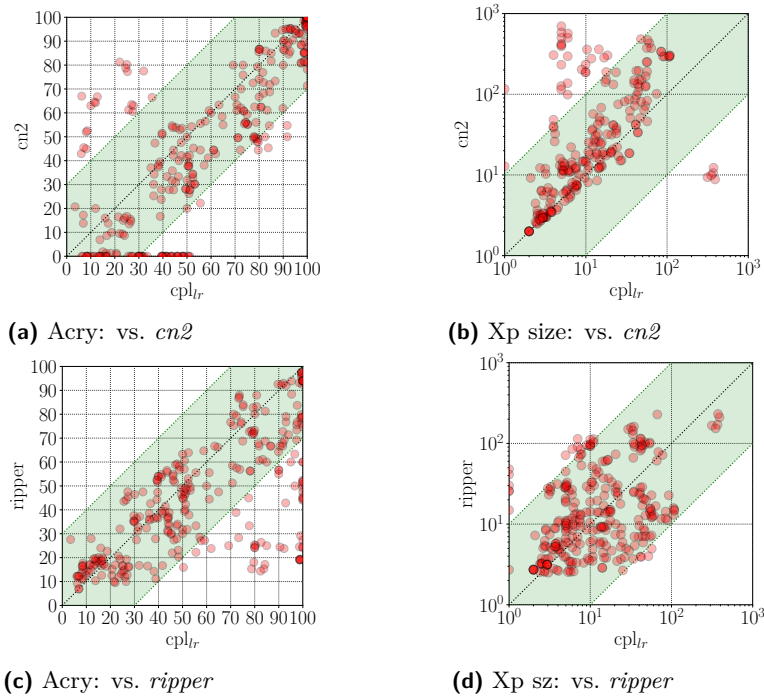


■ **Figure 4** Summary of experimental results when the competitors aim at training a DS given training data \mathcal{E} (i.e. $\mathcal{C} = \mathcal{E}$).

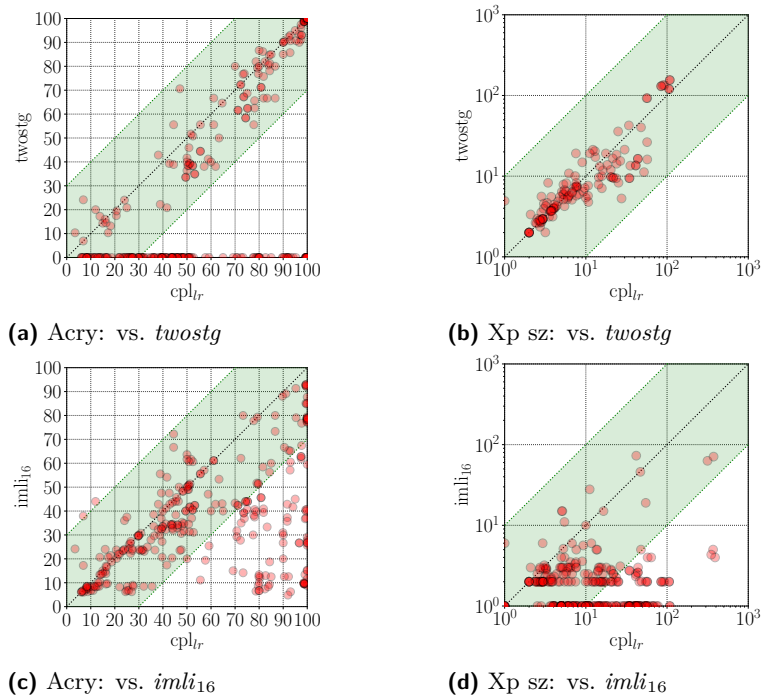
395 within the 3600s time limit. Followed by ids , which solves 166 considered datasets. The
 396 two-stage MaxSAT approach $twostg$ successfully addresses 130 datasets, while the other
 397 MaxSAT algorithm for perfect decision sets opt and its sparse alternative sp_{λ_1} solve 65 and
 398 63 datasets respectively.

399 **Test Accuracy.** The accuracy among the selected approaches is shown in Figure 4b. The
 400 average accuracy among all selected datasets for BTs is 77.34%, beating all DS approaches.
 401 The highest accuracy among DSEs is achieved by all the configurations of the proposed
 402 approach, i.e. cpl and cpl_* , where the average accuracy ranges from 54.01% (cpl_{λ_1}) to
 403 57.49% (cpl_{lr}).⁸ Unsurprisingly, the accuracy in cpl_{λ_1} is lower than the other configurations
 404 since cpl_{λ_1} trades off training accuracy on the number of literals in the computation process.
 405 Next most accurate are the heuristic methods $cn2$ (48.03%) followed by $ripper$ (44.81%).
 406 The average accuracy of $imli_{16}$ and $imli_1$ is 35.47% and 29.7% respectively, while the average
 407 accuracy of $twostg$ is 29.6% and ids is 26.78. Finally, the worst accuracy is demonstrated
 408 by sp_{λ_1} and opt (18.84% and 18.27% on average respectively) as these tools fail to provide

⁸ Note that most datasets we used represent non-binary classification. Also, DSEs are not to be compared with BTs. As Figure 4b shows (and as our work aims to demonstrate), our approach outperforms the state-of-the-art DS inference methods in terms of accuracy.



■ **Figure 5** Comparison of cpl_{lr} vs. $cn2$ and $ripper$ in terms of accuracy and explanation size.



■ **Figure 6** cpl_{lr} vs. $imli_{16}$ and $twostg$ in terms of accuracy and explanation size.

409 prediction information for many datasets within the time limit. We will omit further
 410 discussion of sp and opt_{λ_1} since they solve so few datasets.

411 **Model Complexity.** Figure 4c illustrates the comparison among selected approaches regard-
 412 ing the total number of literals used in each DS solution. The average number of literals are
 413 in order: *imli*₁ (2.77), *imli*₁₆ (8.26), *ids* (21.14), *ripper* (38.47), *cpl*_{l λ 1} (118.47), *cpl*_{l r} (157.53),
 414 *cpl*_l (213.27), *twostg* (265.98), *cpl*_r (584.39) *cpl* (620.82), *cn2* (700.49). Clearly, rule reduction
 415 and literal reduction can significantly reduce the size of the model without significantly
 416 affecting accuracy. Note how our approaches while significantly larger than the least accurate
 417 competitors, are significantly smaller than the most accurate competitor *cn2*.

418 **Explanation Size.** Figure 4d shows the explanation size for each competitor. The aver-
 419 age explanation sizes are in order: *imli*₁ (2.61), *imli*₁₆ (3.00), *cpl*_{l λ 1} (12.14), *ids* (15.28),
 420 *twostg* (17.5), *cpl*_{l r} (25.34), *cpl*_l (26.18), *ripper* (29.08), *cn2* (81.93), *cpl*_r (234.46), *cpl* (240.88).
 421 Figure 4d demonstrates that post-hoc literal reduction not only helps decrease the number
 422 of literals required to explain DS models, but also enables DSes to remain accurate, whereas
 423 rule reduction does not contribute to smaller explanations. With literal reduction applied
 424 our approaches are very competitive in terms of explanation size.

425 **Detailed Comparison.** While cactus plots allow us to compare many methods over a large
 426 suite of benchmarks, they do not allow direct comparison on individual benchmarks. We
 427 provide a detailed comparison of *cpl*_{l r} versus other decision set inference approaches in
 428 Figures 5 and 6, including *cn2*, *ripper*, *twostg*, and *imli*₁₆.⁹ The scatter plots depicting
 429 explanation size are obtained for the datasets solvable by both competitors. Note that *cpl*_{l r}
 430 can generate more accurate DSes than the competitors. Also observe that the explanation
 431 size of DSes computed by *cpl*_{l r} is smaller than *cn2* and comparable with *twostg*. Although
 432 the explanation size of DSes in *cpl*_{l r} is larger than *ripper* and *imli*₁₆, the two approaches are
 433 less interpretable as they compute DSes representing only one class.

434 **Summary.** The experimental results were performed on various datasets, demonstrating
 435 that our approach computes DSes that outperform the state-of-the-art competitors in terms
 436 of accuracy and yield comparable explanation size to them.

437 **6 Conclusions**

438 This paper introduced a novel *anytime* approach to generating decision sets by means of
 439 on-demand extraction of generalized abductive explanations for boosted tree models. It
 440 can be used for exhaustive compilation of a BT model wrt. the entire feature space, or
 441 target a set of training instances. Augmented by a number of post-hoc model reduction
 442 techniques, the approach is shown to compute decision sets that are more accurate than
 443 decisions sets computed by the state-of-the-art algorithms and comparable with them in
 444 terms of explanation size.

445 As the proposed approach targets generating a decision set by compiling a BT, a natural
 446 line of future work is to extend the proposed approach to compile BTs into the other
 447 interpretable models, i.e. decision trees and decision lists, making use of AXp extraction for
 448 BTs. Additionally, another future work is to apply AXp extraction to compile other accurate
 449 black box models, e.g. neural networks, into decision sets.

⁹ The average results across the folds are given in the appendix.

References

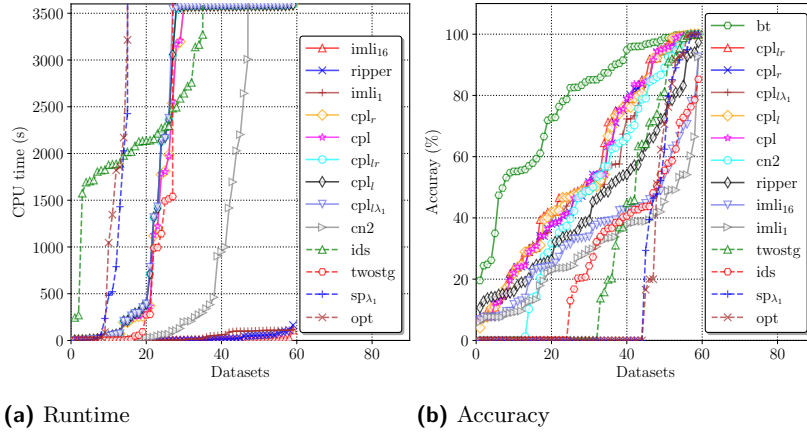
- 450 1 ACM. Fathers of the deep learning revolution receive ACM A.M. Turing award. <http://tiny.cc/9plzpz>, 2018.
- 451 2 Jeremias Berg, Emir Demirovic, and Peter J. Stuckey. Core-boosted linear search for incomplete
452 MaxSAT. In *CPAIOR*, pages 39–56, 2019.
- 453 3 Armin Biere, Marijn Heule, Hans van Maaren, and Toby Walsh, editors. *Handbook of*
454 *Satisfiability*. IOS Press, 2021.
- 455 4 Leo Breiman, J. H. Friedman, R. A. Olshen, and C. J. Stone. *Classification and Regression*
456 *Trees*. Wadsworth, 1984.
- 457 5 Tianqi Chen and Carlos Guestrin. XGBoost: A scalable tree boosting system. In *KDD*, pages
458 785–794, 2016.
- 459 6 Peter Clark and Robin Boswell. Rule induction with CN2: some recent improvements. In
460 *EWSL*, pages 151–163, 1991.
- 461 7 Peter Clark and Tim Niblett. The CN2 induction algorithm. *Machine Learning*, 3:261–283,
462 1989.
- 463 8 William W. Cohen. Fast effective rule induction. In *ICML*, pages 115–123, 1995.
- 464 9 Dheeru Dua and Casey Graff. UCI machine learning repository, 2017. <http://archive.ics.uci.edu/ml>.
- 465 10 Jiri Filip and Tomas Kliegr. Pyids-python implementation of interpretable decision sets
466 algorithm by lakkaraju et al, 2016. In *RuleML+ RR*, 2019.
- 467 11 Nicholas Frosst and Geoffrey E. Hinton. Distilling a neural network into a soft decision tree.
468 In *CEx@AI*IA*, volume 2071 of *CEUR Workshop Proceedings*. CEUR-WS.org, 2017.
- 469 12 Bishwamittra Ghosh and Kuldeep S. Meel. IMLI: an incremental framework for MaxSAT-based
470 learning of interpretable classification rules. In *AIES*, pages 203–210. ACM, 2019.
- 471 13 Jianping Gou, Baosheng Yu, Stephen J. Maybank, and Dacheng Tao. Knowledge distillation:
472 A survey. *Int. J. Comput. Vis.*, 129(6):1789–1819, 2021.
- 473 14 Gurobi Optimization. Gurobi optimizer reference manual, 2022. <http://www.gurobi.com/>.
- 474 15 Laurent Hyafil and Ronald L. Rivest. Constructing optimal binary decision trees is NP-complete.
475 *Inf. Process. Lett.*, 5(1):15–17, 1976.
- 476 16 Alexey Ignatiev. Towards trustable explainable AI. In *IJCAI*, pages 5154–5158, 2020.
- 477 17 Alexey Ignatiev, Yacine Izza, Peter J. Stuckey, and João Marques-Silva. Using MaxSAT for
478 efficient explanations of tree ensembles. In *AAAI*, pages 3776–3785, 2022.
- 479 18 Alexey Ignatiev, Edward Lam, Peter J. Stuckey, and Joao Marques-Silva. A scalable two stage
480 approach to computing optimal decision sets. In *AAAI*, pages 3806–3814, 2021.
- 481 19 Alexey Ignatiev, Antonio Morgado, and Joao Marques-Silva. RC2: an efficient MaxSAT solver.
482 *J. Satisf. Boolean Model. Comput.*, 11(1):53–64, 2019.
- 483 20 Alexey Ignatiev, Nina Narodytska, and Joao Marques-Silva. Abduction-based explanations
484 for machine learning models. In *AAAI*, pages 1511–1519, 2019.
- 485 21 Alexey Ignatiev, Nina Narodytska, and Joao Marques-Silva. On validating, repairing and
486 refining heuristic ML explanations. *CoRR*, abs/1907.02509, 2019. URL: <http://arxiv.org/abs/1907.02509>, [arXiv:1907.02509](https://arxiv.org/abs/1907.02509).
- 487 22 Alexey Ignatiev, Filipe Pereira, Nina Narodytska, and João Marques-Silva. A SAT-based
488 approach to learn explainable decision sets. In *IJCAR*, pages 627–645, 2018.
- 489 23 Yacine Izza, Alexey Ignatiev, and Joao Marques-Silva. On tackling explanation redundancy in
490 decision trees. *J. Artif. Intell. Res.*, 75:261–321, 2022.
- 491 24 Yacine Izza, Alexey Ignatiev, Peter J. Stuckey, and Joao Marques-Silva. Delivering inflated
492 explanations. *CoRR*, abs/2306.15272, 2023.
- 493 25 Yacine Izza and Joao Marques-Silva. On explaining random forests with SAT. In *IJCAI*, July
494 2021.
- 495 26 Anil P. Kamath, Narendra Karmarkar, K. G. Ramakrishnan, and Mauricio G. C. Resende. A
496 continuous approach to inductive inference. *Math. Program.*, 57:215–238, 1992.

- 501 27 Kentaro Kanamori, Takuya Takagi, Ken Kobayashi, Yuichi Ike, Kento Uemura, and Hiroki
502 Arimura. Ordered counterfactual explanation by mixed-integer linear optimization. In *AAAI*,
503 pages 11564–11574. AAAI Press, 2021.
- 504 28 Richard M. Karp. Reducibility among combinatorial problems. In *Complexity of Computer*
505 *Computations*, pages 85–103, 1972.
- 506 29 Himabindu Lakkaraju, Stephen H. Bach, and Jure Leskovec. Interpretable decision sets: A
507 joint framework for description and prediction. In *KDD*, pages 1675–1684, 2016.
- 508 30 Yann LeCun, Yoshua Bengio, and Geoffrey Hinton. Deep learning. *Nature*, 521(7553):436,
509 2015.
- 510 31 Zhendong Lei and Shaowei Cai. Solving (weighted) partial maxsat by dynamic local search
511 for SAT. In *IJCAI*, pages 1346–1352, 2018.
- 512 32 Zhendong Lei and Shaowei Cai. Nudist: An efficient local search algorithm for (weighted)
513 partial maxsat. *Comput. J.*, 63(9):1321–1337, 2020.
- 514 33 Zachary C. Lipton. The mythos of model interpretability. *Commun. ACM*, 61(10):36–43, 2018.
- 515 34 Scott M. Lundberg and Su-In Lee. A unified approach to interpreting model predictions. In
516 *NeurIPS*, pages 4765–4774, 2017.
- 517 35 Chuan Luo, Shaowei Cai, Kaile Su, and Wenxuan Huang. CCEHC: an efficient local search
518 algorithm for weighted partial maximum satisfiability. *Artif. Intell.*, 243:26–44, 2017.
- 519 36 Dmitry Malioutov and Kuldeep S. Meel. MLIC: A MaxSAT-based framework for learning
520 interpretable classification rules. In *CP*, pages 312–327, 2018.
- 521 37 Joao Marques-Silva and Alexey Ignatiev. Delivering trustworthy AI through formal XAI. In
522 *AAAI*, pages 12342–12350, 2022.
- 523 38 Hayden McTavish, Chudi Zhong, Reto Achermann, Ilias Karimalis, Jacques Chen, Cynthia
524 Rudin, and Margo I. Seltzer. Fast sparse decision tree optimization via reference ensembles.
525 In *AAAI*, pages 9604–9613, 2022.
- 526 39 Ryszard S Michalski. On the quasi-minimal solution of the general covering problem. In
527 *International Symposium on Information Processing*, pages 125–128, 1969.
- 528 40 Nina Narodytska, Alexey Ignatiev, Filipe Pereira, and João Marques-Silva. Learning optimal
529 decision trees with SAT. In *IJCAI*, pages 1362–1368, 2018.
- 530 41 Randal S. Olson, William G. La Cava, Patryk Orzechowski, Ryan J. Urbanowicz, and Jason H.
531 Moore. PMLB: a large benchmark suite for machine learning evaluation and comparison.
532 *BioData Min.*, 10(1):36:1–36:13, 2017.
- 533 42 Axel Parmentier and Thibaut Vidal. Optimal counterfactual explanations in tree ensembles.
534 In *ICML*, volume 139 of *PMLR*, pages 8422–8431, 2021.
- 535 43 Marco Túlio Ribeiro, Sameer Singh, and Carlos Guestrin. "why should I trust you?": Explaining
536 the predictions of any classifier. In *KDD*, pages 1135–1144, 2016.
- 537 44 Marco Túlio Ribeiro, Sameer Singh, and Carlos Guestrin. Anchors: High-precision model-
538 agnostic explanations. In *AAAI*, pages 1527–1535, 2018.
- 539 45 Ronald L. Rivest. Learning decision lists. *Mach. Learn.*, 2(3):229–246, 1987.
- 540 46 Cynthia Rudin and Seyda Ertekin. Learning customized and optimized lists of rules with
541 mathematical programming. *Mathematical Programming Computation*, 10:659–702, 2018.
- 542 47 Paul Saikko, Jeremias Berg, and Matti Järvisalo. LMHS: A SAT-IP hybrid MaxSAT solver.
543 In *SAT*, pages 539–546, 2016.
- 544 48 Andy Shih, Arthur Choi, and Adnan Darwiche. A symbolic approach to explaining bayesian
545 network classifiers. In *IJCAI*, pages 5103–5111, 2018.
- 546 49 Dylan Slack, Sophie Hilgard, Emily Jia, Sameer Singh, and Himabindu Lakkaraju. Fooling
547 LIME and SHAP: adversarial attacks on post hoc explanation methods. In *AIES*, pages
548 180–186, 2020.
- 549 50 Jinqiang Yu, Alexey Ignatiev, Peter J. Stuckey, and Pierre Le Bodic. Computing optimal
550 decision sets with SAT. In *CP*, pages 952–970, 2020.
- 551 51 Jinqiang Yu, Alexey Ignatiev, Peter J Stuckey, and Pierre Le Bodic. Learning optimal decision
552 sets and lists with sat. *JAIR*, 72:1251–1279, 2021.

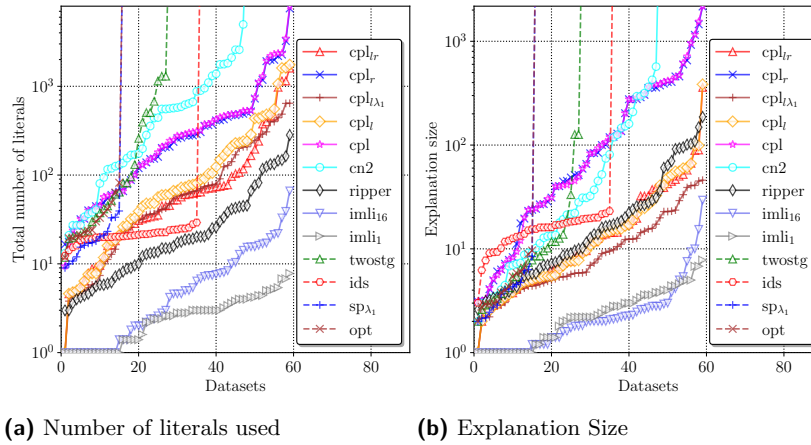
- 553 52 Jinqiang Yu, Alexey Ignatiev, Peter J. Stuckey, Nina Narodytska, and Joao Marques-Silva.
554 Eliminating the impossible, whatever remains must be true: On extracting and applying
555 background knowledge in the context of formal explanations. In *AAAI*, 2023.

556 Appendices

557 **A** Summaries of Results Across Folds

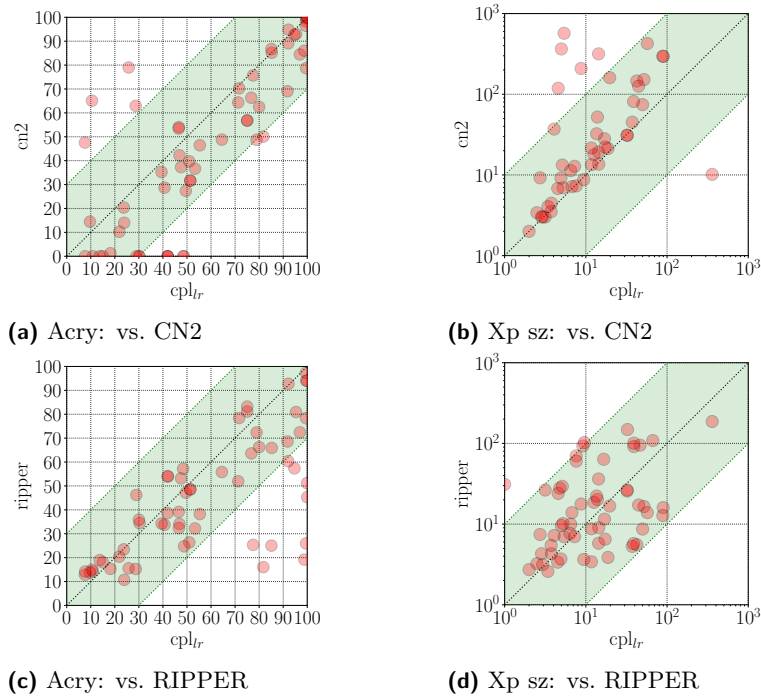


■ **Figure 7** Experimental results of runtime and accuracy across folds.

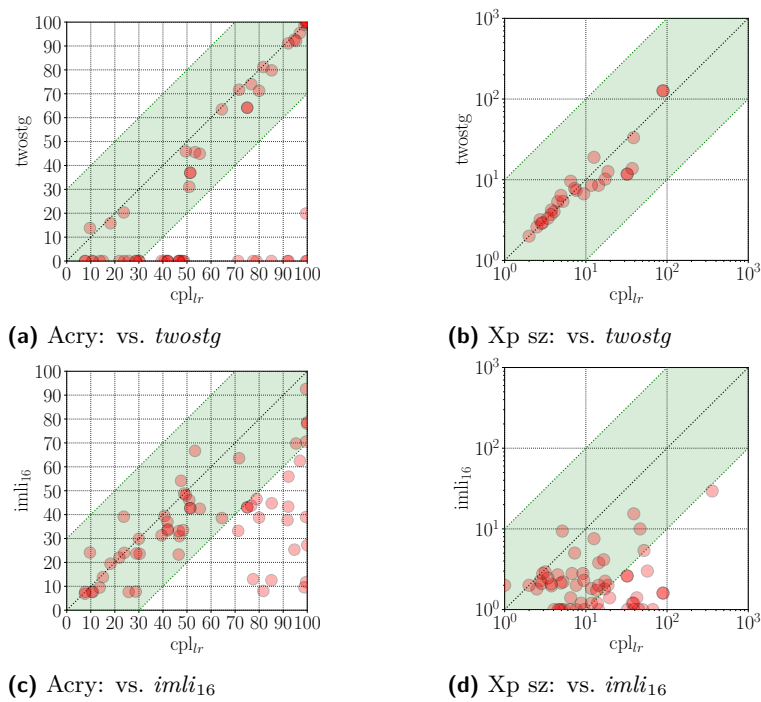


■ **Figure 8** Experimental results of model complexity and explanation size across folds.

558 Figures 7 and 8 illustrate the average experimental results across folds regarding scalability,
 559 accuracy, model complexity, and explanation size. Since 5-fold cross validation is used, these
 560 results for each dataset are obtained from the average of 5 pairs of training and test data.
 561 Here, observations similar to those described in Section 5 can be made, i.e. the best
 562 scalability and accuracy among selected DS competitors are both demonstrated by *cpl* and
 563 *cpl**, $* \in \{l, r, lr, \lambda_1\}$, while *imli*₁ and *imli*₁₆ show the smallest model complexity and
 564 explanation size.



■ **Figure 9** cpl_{lr} vs. CN2 and RIPPER across folds in terms of accuracy and explanation size.



■ **Figure 10** cpl_{lr} vs. $imli_{16}$ and $twostg$ Across Folds in terms of accuracy and explanation size.

565 **B Detailed Comparisons Across Folds**

566 In this appendix, we provide a detailed comparison of cpl_{lr} versus other decision set inference
567 approaches across folds.

568 Figure 9 and Figure 10 detail the comparisons of cpl_{lr} with CN2, RIPPER, $imli_{16}$ and
569 $twostg$ in terms of average accuracy and explanation size across folds. As can be seen in
570 Figure 9a, the accuracy of DSes generated by cpl_{lr} is higher than the accuracy of CN2,
571 where the average accuracy is 57.49% and 48.03%, respectively. Additionally, Figure 9b
572 demonstrate that the explanation size of DSes produced by CN2 (81.93 on average) can be
573 two orders of magnitude larger than the explanation size of cpl_{lr} (25.88 on average).

574 Figure 9c illustrate that the average accuracy in RIPPER is 44.81%, which is 12.68%
575 lower than the accuracy in cpl_{lr} . Although Figure 9d depict that RIPPER is comparable
576 with cpl_{lr} regarding explanation size (29.08 and 25.34 on average respectively), RIPPER is
577 less interpretable as it computes DSes representing only one class.

578 As can be observed in Figure 10a, the accuracy of $twostg$ (29.67% on average) is 27.82%
579 lower than the accuracy in cpl_{lr} while Figure 10b illustrate that the explanation size is
580 comparable between the two approaches. Finally, Figure 10c demonstrate that the accuracy
581 of $imli_{16}$ is 22.02% lower than the accuracy of cpl_{lr} on average. However, as can be seen
582 in Figure 10d, the explanation size of $imli_{16}$ is smaller than the explanation size of cpl_{lr}
583 but $imli_{16}$ generates DSes targeting only a single class, which significantly diminishes the
584 interpretability of computed DSes.